Precision Measurement of $\sin^2\theta_W$ at a Reactor

J. M. Conrad, M.H. Shaevitz

This paper presents a strategy for measuring $\sin^2\theta_W$ to $\sim 1\%$ at a reactor-based experiment, using $\bar{\nu}e$ elastic scattering. This error is comparable to the NuTeV and APV results on $\sin^2\theta_W$, but with substantially different contributions to the systematics. An improved method for identifying $\bar{\nu}p$ events, which are both a background and a normalization sample, is described. The measurement can be performed using the near detector of the presently proposed reactor based oscillation experiments. We conclude that an absolute error of $\sim \delta(sin^2\theta_W) = 0.0020$ may be achieved.

This paper outlines a method for measuring $\sin^2\theta_W(Q^2 = 0)$ at a reactor-based experiment. The study is motivated by the NuTeV anomaly, which is a 3σ deviation from the Standard Model prediction for $\sin^2\theta_W$[1] at $Q^2 = 1$ to 140 GeV^2 ($\langle Q^2_\nu \rangle = 26$ GeV^2, $\langle Q^2_{\bar{\nu}} \rangle = 15$ GeV^2) observed at a deep inelastic neutrino scattering experiment. Other measurements from an array of experiments are in agreement with the Standard Model. These include atomic parity violation[2], which samples $Q^2 \sim 0$; SLAC E158, a Møller scattering experiment at average $Q^2 = 0.026$ [3]; and measurements at the Z-pole with $Q^2 = M_z^2$. Figure 1 summarizes the present state of measurements of $\sin^2\theta_W$. It is important to follow up these results, particularly with an experiment that probes the neutral weak couplings with neutrinos.

The technique uses the rate of the purely leptonic $\bar{\nu}e$ scattering to measure $\sin^2\theta_W$. This signal was first used for such a measurement by Reines, Gurr, and Sobel[5], who found $\sin^2\theta_W = 0.29 \pm 0.05$. The purpose of this paper is to explore what is necessary to improve on their idea and make a competitive measurement today. One important step is to normalize the $\bar{\nu}e$ "elastic scatters" using the $\bar{\nu}p$ "inverse beta decay" events, to reduce the error on the flux. We show that larger detectors, higher flux, and better control of systematics (all of which are available now) also contribute substantial

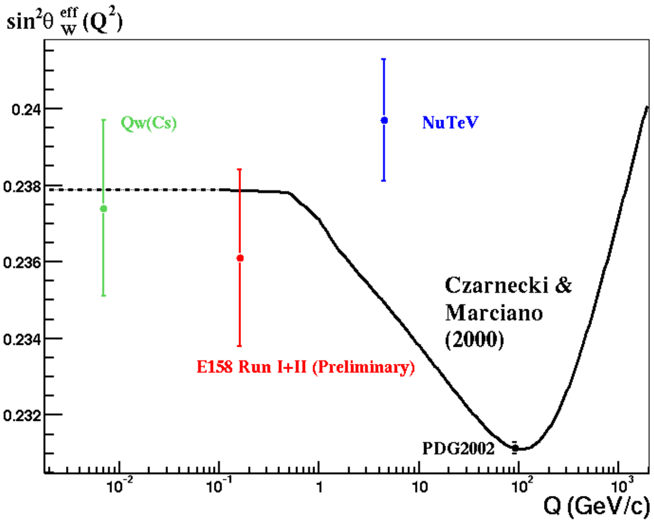

Figure 1: Measurements of $\sin^2\theta_W$ as a function of Q^2; from reference [4]. The curve shows the Standard Model expectation.

improvement. We find that a measurement of $\sim \pm 0.0020$ is achievable. This is comparable to the NuTeV error of ± 0.0017.

The purpose of this paper is to establish that this analysis is worth pursuing at a reactor-based experiment. Thus the analysis is presented in sufficient detail to address the major questions. However, many detailed studies remain to be done. This work serves only as a proof-of-principle.

This discussion is within the context of a spherical scintillator-oil detector. Our "generic design" is similar to CHOOZ[6] and to experiments which are being proposed to measure the oscillation parameter θ_{13}[7]. It consists of a spherical central region of Gd-doped scintillator. The radius of the central region is 190 cm; for this analysis, however, the fiducial volume will be confined to 150 cm. This is surrounded by an undoped scintillator region which extends to a radius of 220 cm. This, in turn, is surrounded by a pure-oil region out to a radius of 290 cm, which acts as a buffer between the active detector and the phototubes. These detectors are optimized to reconstruct $\bar{\nu}p$ events, which dominate the rate when the reactor is running. The detector must be located beneath an overburden of at least 300 mwe (meters, water-equivalent). We show below, first through back-of-envelope arguments, and then through detailed calculation, that this type of detector also suffices for a $\sin^2\theta_W$ analysis.

This paper is organized in the following manner. First, we identify the important questions which drive the design choices. Second, we provide details of the generic experiment used for estimates. Third, we discuss $\bar{\nu}e$ event identification and rates. Fourth, we discuss rejection of $\bar{\nu}p$ events. Fifth, we consider backgrounds produced by natural radioactivity and cosmic rays. Sixth, we consider the errors on the $\bar{\nu}p$ normalization sample. Lastly, we discuss how we find the error on $\sin^2\theta_W$.

1 Introduction to the Design Issues

NuTeV has made a 0.75% measurement, including statistics and systematics, of the weak mixing angle. To match this at the reactor experiment, one needs to measure the $\bar{\nu}e$ absolute rate with a 1.2% uncertainty. In order to establish the design for this experiment, the following questions must be explored:

1. Are there sufficient elastic scattering events to perform this measurement?

2. Can the environmental backgrounds be controlled?

3. Can the elastic scattering events be isolated from the inverse beta decay events?

4. How well can the anti-neutrino flux be known?

This section provides back-of-envelope answers to establish that an error on $\sin^2\theta_W$ comparable to NuTeV is feasible. The purpose is to provide simple motivation for the major cuts, which are summarized in table 1. Details are provided in the later sections.

1.1 Statistics

A 1% statistical error, corresponding to 10,000 elastic events is a necessary goal. In order to see that this can be attained, we can scale from the ratio of elastic events to inverse beta decay. Figure 2 (left) compares the cross sections for these interactions. Figure 2 (right) compares the number of events of each type which will be produced. At low energies, where $\bar{\nu}p$ is kinematically

Cuts, all samples	Range Retained	Primary Motivation
Fiducial volume	40 cm inward from Gd boundary	maintain high n efficiency.
Michel Look-back Boron Look-back	no cosmic for past 22μsec no cosmic for past 4ms	eliminate Michel electrons eliminate ^{12}B beta decays
Cuts, elastic scattering sample	**Range Retained**	**Primary Motivation**
Minimum visible energy Maximum visible energy	> 3 MeV < 5 MeV	Reduce U, Th backgrounds Reduce environmental & $\bar{\nu}p$ backgrounds
Neutron capture energy & delay window	$< 1.8 MeV$ in $0.5 < \Delta T < 200\mu$s	identify and cut $\bar{\nu}p$
Event Topology Analysis	$\Delta^2 < 0.0525$	Reduce $\bar{\nu}p$ background
Cuts, normalization sample	**Range Retained**	**Primary Motivation**
Neutron capture energy & delay window	$E > 5$ MeV $0.5 < \Delta T < 200\mu$s	Isolate well-identified events to maximize n id purity
Event Topology Analysis	$\Delta^2 > 0.065$	Isolate pure $\bar{\nu}p$ events for Gd ratio study

Table 1: General motivation for the major cuts. Visible energy refers to the measured energy of the primary interaction. The event shape analysis exploits the multiple interaction vertices from $\bar{\nu}p$ events, as described in section 4.5

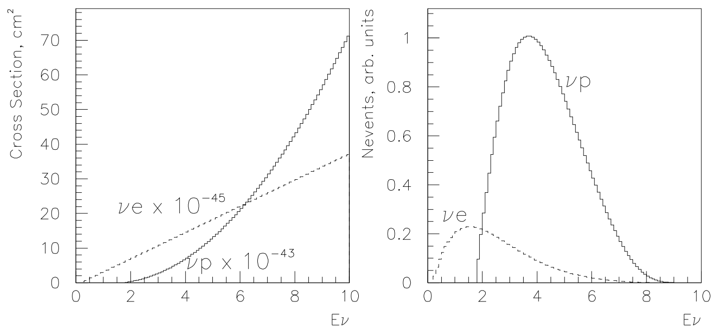

Figure 2: Left: Comparison of νe and νp cross sections as a function of neutrino energy in MeV. Right: Comparison of event rates for νe and νp as a function of neutrino energy in MeV. Note that there are 4.3 more electron targets than free proton targets in the oil.

suppressed, elastic scattering dominates. However, as discussed later, it will be necessary to cut on a "visible energy," the measured energy of the primary interaction, of 3 MeV to remove environmental backgrounds. From Figure 2, one can see that if $> 1 \times 10^6$ $\bar{\nu}p$ events can be collected, then the necessary statistical precision can be reached.

We can use the CHOOZ experiment to argue that this $\bar{\nu}p$ rate is feasible. CHOOZ observed ∼3000 inverse beta decay events in a 5 ton detector located 1 km from two 4.5 GW reactors, running for 132 days effective full power [6]. Using one of the proposed near detectors for the oscillation experiments [7], this rate is substantially improved. These detectors are typically located about 200 m from the reactor, gaining a factor of 25 from solid angle. The detector can be built with increased fiducial mass and still fit within a standard-size tunnel. Multiple detectors can be built. The experiment can feasibly run longer. In summary, the necessary event rate appears to be attainable.

1.2 Environmental Backgrounds

Radioactive backgrounds can be reduced to a tolerable level. Background from natural radioactivity can largely be cut by a visible energy window. However, muon-induced isotopes are among the largest background in this analysis.

Environmental radioactivity in the detector represents a serious background before cuts. However, such sources of background can be rendered negligible by spatial and energy cuts. Activity from the tank walls and phototubes can be removed by fiducial volume cuts. For example, CHOOZ employed a $d > 30$ cm cut from the geode (outer wall) boundary [6]. Background from U and Th dissolved in the scintillator can be removed from the sample through a 3 MeV cut on visible energy, as seen in Figure 3. However, this figure makes clear that excellent energy resolution is a priority, since the cut is near the boundary.

This cut can be introduced without compromising the required statistics for the signal. Unlike a neutrino magnetic moment analysis[8], which is often the goal for elastic scattering studies at reactors, the measurement of $\sin^2\theta_W$ does not rely on low visible energy events. In fact, we will show in section 3 that the sensitivity is enhanced upon increasing the cut on visible energy. Thus, the analysis will require visible energy $>$ 3 MeV. We also cut far from the tank walls, thereby removing this background while enhancing the

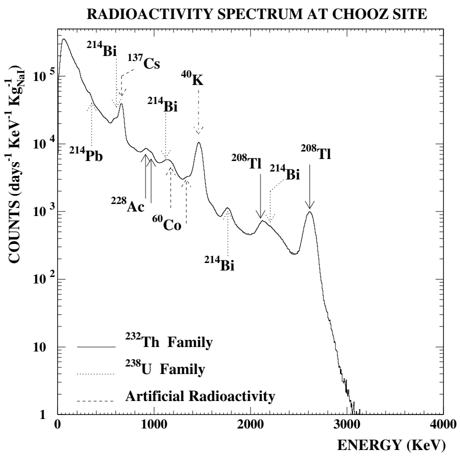

Figure 3: Visible energy from environmental radioactivity measured in the CHOOZ detector hall using a NaI crystal, from reference [6].

sensitivity.

Potential background from cosmic rays comes from the muons themselves, spallation neutrons, Michel electrons from muon decays, and isotopes generated by the muons. From CHOOZ, the cosmic ray flux at 300 mwe was $0.4/\mathrm{m}^2/\mathrm{s}$ [6]. Muons which enter the tank will be easily identifiable through the combination of hits in the veto and light in the tank. A muon will deposit about 2 MeV/cm. Thus cosmic ray events which penetrate into the central region will not survive a 5 MeV maximum visible energy cut. Because these events are easily separated from other backgrounds, the proposed look-back systems discussed below can rely on vetoing only if there is a cosmic ray event.

Spallation neutrons which are unassociated with a cosmic ray have two sources. They may be produced outside of the tank and then enter; or they may be produced by high energy muon interactions with the ^{12}C within the tank, but not be associated with the parent cosmic due to a late capture time. In either case, the neutron capture will fail the $3 < E_{vis} < 5$ MeV window, since captures on Gd produce > 5 MeV and captures on H produce 2.2 MeV. For the case of incoming neutrons, a 40 cm Gd-doped buffer region surrounding the fiducial region will provide further protection from this background.

Few Michel electrons from stopped muon decay will fall within this energy window. These can also be removed via a look-back system which connects a cosmic signal with the following Michel over 10 lifetimes, or 22 μsec. This has a negligible effect on the deadtime.

Production of isotopes by cosmic ray muons produces the most significant backgrounds. Stopped muon capture results in ^{12}B which β decays with a peak at 10 MeV. In order to reduce this background, we will introduce a 40 ms look-back for a parent cosmic ray, introducing an 11% deadtime. Also, isotopes which β decay are produced by high energy cosmic rays interacting with the ^{12}C in the detector. Those with energy above 3 MeV are ^{9}Li, ^{8}He, ^{8}Li , ^{9}C , ^{8}B, all of which have endpoints above 10 MeV; and ^{6}He, which has an endpoint at 3.5 MeV. Introducing the energy window reduces these rates by 80 to 90% depending on the isotope. We will show that these isotopes represent a substantial background, roughly equally divided between the muon capture and the spallation sources.

Based on the above arguments, if one introduces a $3 < E_{vis} < 5$ MeV window, the environmental backgrounds can be controlled, assuming a 300 mwe overburden. We will show that a shallower depth renders the experiment insensitive.

1.3 $\bar{\nu}p$ Mis-identification

Inverse beta-decay events will dominate the rate above 3 MeV. As a start, assume 1×10^6 events are collected. The best handle for separating these events from elastic scatters is observation of the signal from neutron capture. In the case where the neutron is outside of the capture time window, the $3 < E_{vis} < 5$ MeV window aids in reducing the event rate.

If we define our fiducial region as 40 cm within the Gd-doped central detector, n capture will be nearly 100% efficient. However, only 84% of of the events will capture on Gd, producing γ's of > 5 MeV. The remaining 16% capture on H, producing only a single γ of 2.2 MeV. The CHOOZ trigger was insensitive to the captures on H. That is unacceptable for this experiment, since it would lead to 1.6×10^5 mis-identified events. At the end of the run, CHOOZ studied a neural net trigger for H-capture identification which they estimated to be about 90% efficient for triggering on captures [9]. It is straightforward to improve this efficiency by extending the search radius around the neutrino vertex, as long as the trigger rate from accidental coincidences can be handled. As discussed in section 2, we assume that this efficiency can be improved to better than 99% by extending the search region.

The search for a neutron candidate is performed within a time window following the neutrino interaction. CHOOZ used 2 to 100 μs [6]. Given a neutron 30 μs capture lifetime, one would naively think that 6% of the neutrons would capture before 2μs. However, this is not true because the neutron must first thermalize before capturing. The CHOOZ inefficiency due to the time window was due to about 3% early and 3% late captures. As discussed in section 4, events with neutrons outside of the time window tend to also be outside of the visible energy window. We assume that in a new experiment it is feasible to open the time window earlier and end the window later, further reducing this background rate.

For further improvement, we explore an analysis based on the distribution of electromagnetic vertices in the event. For $\bar{\nu}p$ events, one expects multiple vertices due to the Compton scatters of the photons produced by the annihilation of the positron. On the other hand, $\bar{\nu}e$ events have only a single source for photon production. This "event topology analysis" is preliminary, therefore we present results with and without an event topology cut applied.

1.4 Normalization

Absolute knowledge of the reactor neutrino flux is limited by the $\sim 2\%$ uncertainty on the reactor isotope content. To avoid this error, we use $\bar{\nu}p$ events to establish the normalization for the $\bar{\nu}e$ events. The statistical error on the $\bar{\nu}p$ events is negligible since there are $\sim 1 \times 10^6$ events expected. Thus, systematics associated with this sample will dominate the measurement. The cross section for $\bar{\nu}p$ is well-predicted, as discussed in section 4, so this systematic error is negligible. An important systematic error comes from determination of the ratio of targets for $\bar{\nu}e$ versus $\bar{\nu}p$ scatters, *i.e.* the electron-to-free-proton ratio. CHOOZ achieved approximately 0.8% error on their free proton content, which translates into a 0.6% error on the electron-to-free-proton ratio. Another important systematic question is related to the n-identification. One can obtain a very pure sample of $\bar{\nu}p$ events by requiring a Gd capture. However, this will introduce a systematic error from the ratio of Gd captures to the total, which was 1% in CHOOZ. This is unacceptably high for this analysis and must be reduced through a combination of improved calibration studies and a possible event topology analysis. Alternatively, assuming we can trigger with high efficiency on events with H captures, one can accept all n-identified events into the $\bar{\nu}p$ sample. This eliminates the error on the

Gd capture ratio but introduces possible backgrounds from accidental coincidences. Estimating these backgrounds will require a detailed study, beyond the scope of the present work. Therefore, for this analysis, we will use the former method of identifying a clean sample through the Gd captures.

2 The "Generic" Detector

For the initial discussion we used a "generic" set-up which is drawn from the Braidwood design for the θ_{13} experiment. We assume two 3.6 GW reactors. The neutrino flux is taken from reference [10]. The detector hall is 224 m from the two reactors and beneath 300 mwe of overburden. Data taking is assumed to be 900 live-days. Given an 11% deadtime, as discussed below, this corresponds to 1000 calendar days. Two spherical detectors with active veto shielding are envisioned. Table 2 summarizes the assumptions we make about the detectors. The detectors also have passive shielding.

Two detectors are required to attain the necessary fiducial volume while allowing the detectors to fit within a 3 m radius tunnel. Each has a "central region" of Gd-doped scintillator. The outer radius of this region is 190 cm. To maximize the signal efficiency and minimize backgrounds, the fiducial radius for the analysis is taken to be 150 cm. The Gd-doped region is surrounded by a 30 cm "photon catcher" of scintillator with no Gd doping. These two regions are, in turn, surrounded by an oil "buffer" in which the phototubes are immersed. The buffer region extends to a 290 cm radius. Hence the phototubes are located 100 cm from the central region and 150 cm from the fiducial region.

The scintillator in both the central and photon catcher regions will be at the 20% to 30% level and have a time constant of $\sim$3 ns. This design is expected to have good vertex and energy resolution. There is no angular measurement for the outgoing lepton because the tracks are quite short and the isotropic scintillation light obscures any directional Cerenkov light. The attenuation length of the scintillator regions is assumed to be 4 m, as compared to 15 m in the undoped buffer.

We will assume that 200 photoelectrons per MeV are detected. This is similar to the CHOOZ design[6] and is a factor of two less than the Borexino test detector, CFT [11]. CHOOZ achieved an energy resolution of 0.33 MeV at 8.1 MeV [6]. The CFT detector used α-decays with a corresponding electron-like energy of 862 keV to show that, in the central region of the

Radius of fiducial region	150 cm
Fiducial volume per detector	13 tons
Outer radius of central region	190 cm
Tonnage of the central region	26.5 tons
Outer radius of photon catcher	220 cm
Outer radius of detector	290 cm
Energy resolution	not considered
Vertex resolution	4 cm
e^- and e^+ tracklength	negligible
n capture pathlength	6 cm
0.5 MeV γ Compton pathlength	11 cm
att. length of photons in central region & photon catcher	4 m
att. length of photons in pure oil	15 m
Fraction of n from $\bar{\nu}p$ events which escape detector	0%
Fraction of photons from positron annihilation which escape	0%
Fraction of n which capture on Gd	84%
Neutron capture time	30.5μs
Neutron-delay requirement efficiency	97%
Fraction of nGd captures which are reconstructed	100%
Error on nGd capture ratio (from ^{252}Cf study)	0.7%
Fraction of n which capture on H	16%
Search window for capture on H	30 cm
Fraction of nH capture events which trigger	99.4%

Table 2: Assumptions related to the generic detector used in this paper. See the text for justification. Note that two detectors are proposed for the experiment.

detector, energy resolution of 4-5% is attainable. For this analysis, we do not consider effects due to energy resolution. Instead, we make generous energy cuts so as to avoid issues of energy smearing.

The vertex resolution on the neutrino interaction is taken to be $\sim$4 cm. This is consistent with CHOOZ laser flasher studies [6]. CFT obtained a similar resolution using an alpha source, with equivalent energy of 0.862 keV [11]. We assume 4 cm resolution on all γ, electron and positron events. We assume that the pathlength of an electron or positron in oil is negligible, thus vertices are "point-like."

In order to identify $\bar{\nu}p$ events, which represent both a background and a normalization sample, the signal from the neutron capture is used. In Gd-doped scintillator, the pathlength for a thermal neutron is 6 cm; the fiducial volume cut of 40 cm from the central region edge represents 6.7 pathlengths. As a result, <0.15% of the neutrons produced at the edge of the fiducial volume will escape. This results in a negligible loss rate and so we round to 100% efficiency for capture of neutrons produced by $\bar{\nu}p$ interactions.

Neutron capture is time-delayed with respect to the positron track, with a capture time of 30.5μs [6]. We will apply a time window of $0.5 < \Delta t < 200\mu$s, which is wider then the CHOOZ neutron delay time window discussed in section 1. This results in $< 3\%$ failure in associating a neutrino vertex due to early captures and 0.1% failures due to late captures. We will address how these events can be removed in section 4.

Gd doping results in a cascade of photons resulting in 5 to 8 MeV when the neutron captures. Due to the excellent energy resolution, we will assume that 100% of these photons can, in principle, be observed. ¿From reference [6], the percentage of events which capture on Gd is 84%. In CHOOZ, the 1% error on this percentage comes from the statistics on capture studies using a radioactive source. Because we will run for twice the CHOOZ period, this error can be reduced to 0.7%. This is still high and must be improved. A possible method is discussed in section 4.5.

The remaining 16% of neutrons will capture on hydrogen, resulting in a single 2.2 MeV γ. In this analysis, it is necessary for a large fraction of these events to be identified using a combination of timing and position. CHOOZ studied a trigger[9] for the H capture events, but this was developed late in the experiment and not implemented before data taking ended. The trigger was based on a neural net. Loosely translating to simple cuts, this trigger used a 14 cm search radius around the neutrino vertex and a window of $\pm$0.5 MeV. The inefficiency in this trigger was dominated by the search radius,

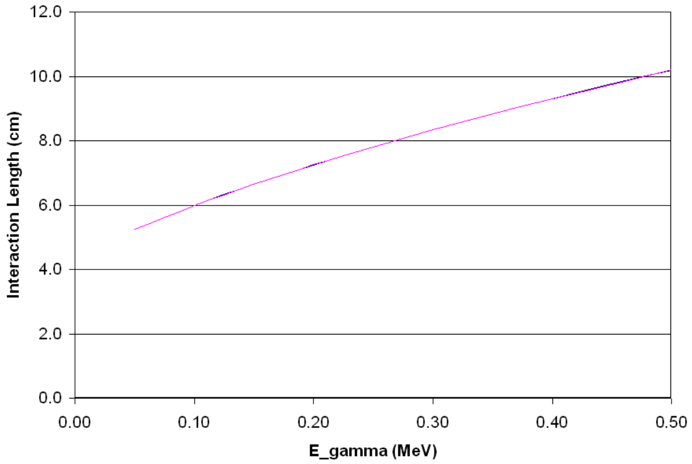

Figure 4: Compton length as a function of photon energy.

because 9.7% of events survive without interacting within this range. The singles rate in CHOOZ demanded this small radius. However, this singles rate was dominated by events coming from the tank walls because there was no pure oil buffer. The pure-oil buffer planned in this experiment should significantly reduce this rate and allow an expanded search window.

KamLAND quotes an efficiency for $\bar{\nu}p$ events of 78±1.6%[12]. This experiment is performed on oil with no Gd doping, thus the n pathlength is large. The inefficiency is again largely driven by the cut on relative position of the neutrino and neutron vertex. Because the inefficiency for triggering on H capture is largely due to the 14 cm search window used in the CHOOZ neural net trigger, we propose to increase the search window in the new experiment to 30 cm. This yields a 0.6% inefficiency.

The inverse beta decay events also produce two 0.5 MeV photons when the positron annihilates. In a later section, we will show that these photons will provide a useful second method for tagging $\bar{\nu}p$'s. These photons lose energy through Compton scatters, with a path length in CH_2 of $\sim$ 11 cm (see Figure 4). While the Compton peak is at $2/3E_\gamma$, note that the average energy loss is $1/3E_\gamma$. Thus an event can be expected to have several Compton scatters before exiting the detector. The "photon-catcher" region and the Gd-doped region are used to reconstruct the energy of an event. With the 1.5

m radius fiducial volume cut, this places a 0.5 MeV photon 6.5 pathlengths from the inactive oil-buffer region. The resulting inefficiency of 0.15% on photon reconstruction is rounded to zero for the discussion below. In other words, we assume 100% of the photons at 0.5 MeV will be contained.

As per reference [7], U and Th concentrations in the scintillator are 100 times higher than the expectation for Borexino. Other radioactive contaminants, such as ^{14}C are not considered because the visible energy from these decays is far below the energy level of this study.

As described in section 1, cosmic ray background must be reduced for this analysis. We assume the detector overburden to be 300 mwe, yielding a cosmic ray flux of 0.4/m^2/s at CHOOZ[6]. Given the proposed generic design, which has 2 detectors each with a 1.5 m radius of active area for cosmic rays, the rate will be 2.8 Hz per detector. Each detector will have a veto detector, which can be designed with $> 99.99\%$ efficiency as achieved in MiniBooNE [13]. However, for this analysis, the detector itself can also be used as the veto, allowing for highly improved cosmic ray identification. Cosmic ray muons which enter the active areas (the photon catcher and the central region) will deposit about 2 MeV/cm yielding 0.4 hits/cm/phototube, or 12 hits/phototube for muons which radially traverse the photon catcher. For this discussion, we will assume that all cosmic ray muons are potentially identifiable in either the veto or the main detector and have characteristics which allow them to be separated from other sources of background.

Two look-back systems are employed at the analysis level, not the trigger level. In order to tag the Michel electrons from stopped cosmic rays, we will use a look-back-system of 10 lifetimes (22μs). This represents a negligible deadtime. In order to tag ^{12}B decays, a 40 ms look-back is introduced. This results in an 11% deadtime. Thus for 900 days of live-time, this analysis requires 1000 calendar days of running.

3 $\bar{\nu}e$ Event Rate and Identification

$\bar{\nu}e$ events result either from scattering via exchange of a Z boson or annihilation via exchange of a W boson. The differential cross section for $\overline{\nu}_e e^-$

scattering is:

$$\frac{d\sigma}{dT} = \frac{G_F^2 m_e}{2\pi}\left[(g_V+g_A)^2+(g_V-g_A)^2\left(1-\frac{T}{E_\nu}\right)^2+(g_A^2-g_V^2)\frac{m_eT}{E_\nu^2}\right] + \frac{\pi\alpha^2\mu_e^2}{m_e^2}\frac{(1-T/E_\nu)}{T}$$

where E_ν is the incident $\overline{\nu}_e$ energy, T the electron recoil kinetic energy, and the couplings are given by

$$g_V = 2\sin^2\theta_W + \frac{1}{2} \qquad g_A = -\frac{1}{2}$$

The term in brackets is the weak interaction contribution and the last term gives the contribution from electromagnetic scattering if the neutrino has a magnetic moment, μ_e.

The total visible energy, E_{vis} in elastic scatters is the kinetic energy of the e^-, T. This is in contrast to $\bar{\nu}p$ events where additional visible energy will come from both the positron annihilation and also the neutron capture.

If one could reconstruct both T and E_ν in $\bar{\nu}e$ events, then an analysis of T/E_ν dependence would be attractive. This method evades the issue of absolute normalization. However, in the generic detector described above the angle of the e^- cannot be reconstructed. Therefore, only T is measurable. Once this cross section is folded with the reactor flux, the variation of the shape versus T is insensitive to $\sin^2\theta_W$.

On the other hand, the total rate of $\bar{\nu}$ events is sensitive to $\sin^2\theta_W$. In fact, the sensitivity to $\sin^2\theta_W$ can be enhanced by introducing a cut on T. Integrating over the recoil electron kinetic energy from $T_{\min}$ to $T_{\max}$ gives a cross section as a function of E_ν given by

$$\begin{aligned}\sigma_{T_{\min}\text{ to }T_{\max}} &= \frac{G_F^2 m_e}{2\pi}\Big[\left((g_V+g_A)^2+(g_V-g_A)^2\right)(T_{\max}-T_{\min}) \\ &\quad +\frac{1}{2}\left(\frac{m_e\left(g_A^2-g_V^2\right)}{E_\nu^2}-\frac{2(g_V-g_A)^2}{E_\nu}\right)(T_{\max}^2-T_{\min}^2) \\ &\quad +\frac{(g_V-g_A)^2}{3E_\nu^2}(T_{\max}^3-T_{\min}^3)\Big]\end{aligned}$$

T in the range of 2.5 to 5 MeV is optimal. However, as discussed in section 1, cuts on various backgrounds dictate $3 < (T = E_{vis}) < 5$ MeV.

4 The $\bar{\nu}p$ Background

A major potential source of background comes from misidentified $\overline{\nu}_e p \to e^+ n$ events. The cross section is given by

$$\sigma\left(E_{e^+}\right) = \frac{2\pi^2}{m_e^5 f \tau_n} p_{e^+} E_{e^+}$$

where $E_{e^+}(p_{e^+})$ is energy(momentum) of the outgoing positron, $f = 1.71465(15)$ [10, 6] is the free neutron decay phase-space factor, and $\tau_n = 886.7 \pm 1.9$ s [14] is the neutron lifetime. Using these measurements of f and τ_n, one finds that the cross section is known to the 0.2% level. Thus the cross section is very well known. For this process, the $E_{\overline{\nu}_e}$ energy threshold is 1.804 MeV and the incoming $\overline{\nu}_e$ energy is simply related to the outgoing positron energy by

$$E_{\overline{\nu}} = E_{e^+} + (M_n - M_p) = E_{e^+} + 1.2933 \text{ MeV}$$

Most $\bar{\nu}p \to e^+ n$ are identified by the outgoing n. However, the n may not be observed because of the the 0.6% inefficiency on identifying H capture or because the neutron was outside of the neutron-delay time window. In the latter case, $< 3\%$ of the neutron capture signals occur early and will be included in the visible energy associated with the neutrino vertex. Also, 0.1% of the neutrons will capture late, leaving a primary neutrino vertex and a secondary neutron vertex which is mistakenly "unassociated." Primary $\bar{\nu}p$ vertices with no associated neutron signal can be identified using by an analysis which exploits the diffuse tertiary vertices from the γ's produced by positron annihilation. We call this an "event topology analysis," because it distinguishes between point-like source shapes and diffuse source shapes in the tank.

4.1 Rejection Through n Identification

Most $\bar{\nu}p$ events can be rejected through identification of the time-delayed n. We take the efficiency for reconstructing the photons from Gd-capture to be 100%. On the other hand, the efficiency for identifying the photon associated with H capture is only 99.4%. Thus the total n-identification efficiency is $0.84 + (0.16 \times 0.994) = 0.999$. This is to say, 0.1% of n events that had a sufficient time offset will fail to be identified.

The systematic error on this is small. The error on the Gd capture fraction is assumed to be 0.7% (see section 2. The Gd capture fraction introduces an error, δ, which changes the efficiency to $\epsilon = (0.84 + \delta) + (0.16 - \delta) \times 0.994$. Taking the derivative, $d\epsilon = .006 d\delta$. If we can measure δ to 0.007, then this implies an error of 4×10^{-5}. The 0.006 inefficiency on H capture comes from neutrons which exit the 30 cm search region. In this case, using binomial statistics, one needs 17,000 tagged calibration-source events in order to obtain a 10% error on this inefficiency. We believe this can be achieved. Therefore, we assume zero systematic error.

4.2 Rejection Through an E_{vis} Cut

In the case of $< 3\%$ of the events, the neutron capture occurs earlier than the neutron delay time window. Most of these events can be removed from the sample by applying the $3 < E_{vis} < 5$ MeV cut. To see this, first consider events which capture on Gd. These will deposit ~ 8 MeV, which will cause the total visible energy to exceed the window. On the other hand, some of the 16% of events which capture on H can contribute to the background. In these events the neutron releases 2.2 MeV and the positron annihilation releases 1 MeV. Thus the minimum visible energy for $\bar{\nu}p$ with H capture is 3.2 MeV. Events with up to 1.8 MeV in positron kinetic energy will be within the visible energy window. 20% of $\bar{\nu}p$ events will have positron kinetic energy in this range. Thus the upper limit on this background, which was 3%, is reduced by the factor 0.16×0.20 to 0.1%. We again assume the systematic error on this is sufficiently small to be neglected in this discussion.

4.3 Unassociated Positrons Due to Late Neutron Capture

In 0.1% of $\bar{\nu}p$ events, the neutron capture is late. This results in a positron which has no associated neutron tag, and thus is a background.

The total visible energy for an unassociated positron is the kinetic energy of the lepton plus 1 MeV from the positron annihilation. Approximately 60% of the unasociated positron events fall within the $3 < E_{vis} < 5$ MeV window. Thus this background is reduced to 0.06%. Again we assume no appreciable systematic error on this value.

4.4 Unassociated (Late) Neutrons

In the 0.1% of $\bar{\nu}p$ events, where the neutron capture is late, the unassociated neutron could potentially produce a background. For the case where the neutron is early, the events will be removed in the event topology analysis described above. In the case of a neutron capture which is late, the neutron will not be properly associated with the neutrino vertex. These unassociated neutrons will appear to be a single vertex. However, those which capture on H will produce a 2.2 MeV γ and those which capture on Gd will produce > 8 MeV visible energy. Therefore, the background from unassociated neutrons will be negligible.

4.5 Rejection Through an Event Topology Analysis

At this point, three types of events escape identification:

1. Events in the neutron delay time window which fail to have a reconstructed capture: 0.1% (see section 4.1).

2. Events with an early neutron capture that were not eliminated through the $E_{vis\ max}$ cut: 0.1% (see section 4.2).

3. Events with a late neutron capture and thus have an unassociated positron vertex: 0.06% (see section 4.3).

This yields a total background of 0.26%. Note that, within the $3 < E_{vis} <$ 5 MeV window, we assume, at this point, that $\bar{\nu}e$ reconstruction is 100% efficient.

We use these values to calculate an "upper limit" on the uncertainty which can be achieved in the analysis. We believe further rejection of the above classes of background can be achieved by differentiating between e^- vertices, which are the signal, and e^+ vertices which are the background. The latter will undergo annihilation at the end of the track producing two 0.5 MeV γ-rays. As discussed in section 2, the pathlength for Compton scattering of these γ's is 11 cm. At each scatter, only a fraction of the energy is lost. Thus, the existence of these photons can be inferred if the reconstructed vertex is extended compared to the expectation for an e^- event of the same energy.

We call our identification method an "event topology analysis," because it separates point-like photon source shapes from source regions with extended shape. We can reconstruct events assuming that the shape of the source for the scintillation photons is point-like, such as one expects for $\bar{\nu}e$ events. If, instead, that shape is elongated because this is a $\bar{\nu}p$ event with annihilation photons, then we will obtain a poor fit.

To give a sense of the improvement one might achieve with an event shape analysis, we have developed a toy model. We use these results to set an "aggressive estimate" of the uncertainty in $\sin^2\theta_W$. In our simple Monte Carlo, the characteristics of the detector are defined according to Table 2. We generate 5 MeV events. Vertices are generated as point sources. The charge assigned to each "tube" (*i.e.* location at the wall) is calculated based on solid angle, with correction for attenuation length. Charge is smeared according to a Gaussian of width 10%.

$\bar{\nu}e$ events consist of a single point-source. $\bar{\nu}p$ events have a single central source producing 80% of the hits and a set of sources associated with the annihilation photons. The annihilation photons are generated back-to-back at random angles. The photons Compton scatter, each losing energy up to four times, thereby producing up to eight additional point-sources. The scattering length is adjusted as the photon loses energy, as described in Figure 4. The visible energy deposited for each scatter and the angle of the outgoing photon is determined from the Compton formula.

Figure 5 shows an example $\bar{\nu}p$ event. We focus on the central square meter of the detector. The event was generated at (0,0,0). The box size indicates the amount of charge associated with each vertex. The distribution of charge outside of the central vertex region is evident. These small vertices are the Compton scatters associated with the two annihilation photons.

Events are reconstructed based on total charge. Timing is not considered, although CFT studies indicate that timing can improve the vertex resolution [11]. Reconstruction for this analysis assumes a single vertex. When this Monte Carlo is run on $\bar{\nu}e$ events located at (0,0,0) in the detector the reconstructed vertex distribution has an error of 4 cm, as assumed in section 2.

A "χ^2-like" variable, Δ^2, gives the squared deviation of the charge in the phototubes from the level expected if all hits come from a point source. The distribution is shown in Figure 6. The solid curve is for $\bar{\nu}e$ events. The dashed curve is for $\bar{\nu}p$ events. The curves are well separated. By selecting events with $\chi^2 < 0.0525$, 80% of the $\bar{\nu}p$ events are cut while 85% of the $\bar{\nu}e$ are retained. If the event had also contained a 2.2 MeV photon from a neutron capture, the energy would appear to be even more diffuse and the separation would be more evident.

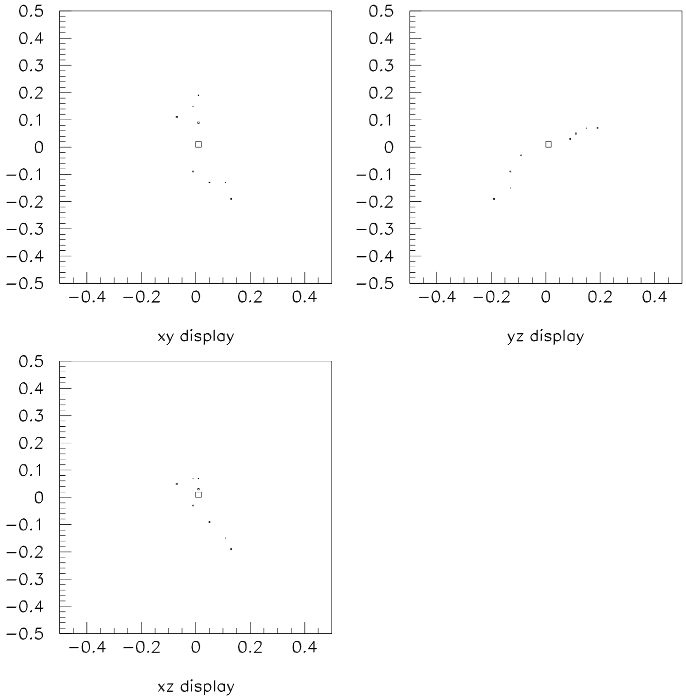

Figure 5: xy, yz and xz views of a simulated $\bar{\nu}p$. Units are in meters. Each box represents an interaction vertex. The size of the box indicates the energy deposited. The neutrino interaction is the large box at (0,0,0). The trail of interactions of the 0.5 MeV photons which Compton scatter is visible.

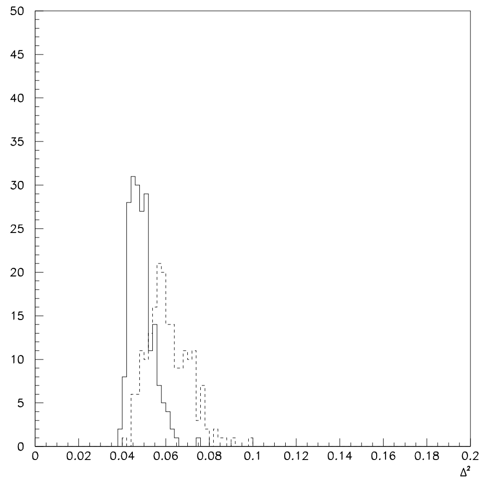

Figure 6: Squared difference between the expected charge and the observed charge. Solid: $\bar{\nu}e$ events; Dash: $\bar{\nu}p$ events.

This event topology analysis is a simple model which is meant to serve as a proof-of-principle. It is clear that both the idea and the Monte Carlo can be honed. For example, one could also fit the sample for multiple vertices and combine the results into a likelihood. Also, incorporating information on the positron annihilation lifetime in liquid scintillator may improve this technique [15]. However, for this discussion, we apply the results of the simple model and do not assume any improvement.

After applying the 80% reduction factor on the vertex identification one finds:

1. Events in the neutron delay time window which fail to have a reconstructed capture: 0.02%.

2. Events with an early neutron capture that were not eliminated through the $E_{vis\ max}$ cut: 0.02%.

3. Events with a late neutron capture, hence an unassociated positron: 0.01%.

The total is: 0.05%. Application of the event topology analysis reduces the efficiency for $\bar{\nu}e$ reconstruction to 85% within the visible energy window.

Therefore, we assume that if an event topology analysis is applied, the run will be extended by 15% to 1035 live-days to make up for the loss in statistics.

5 Environmental Backgrounds

Section 1 introduced the environmental backgrounds which are faced in reactor experiments. They come largely from uranium and thorium contaminants, Michel electrons, spallation neutrons, and muon-produced isotopes. In this section, we show that the $3 < E_{vis} < 5$ MeV window, in combination with the cosmic-ray look-back systems proposed in section 2, reduce most environmental backgrounds to a negligible level, however 11,200 events result from muon interactions, with 3100 coming from ^{12}B and 8100 coming from spallation-produced isotopes. In the case where an event topology analysis is considered, this rate is increased by 15% to account for the extra run time.

5.1 U and Th Backgrounds

The bulk of the naturally-occurring radioactivity in the region of interest comes from U and Th decay chains. As an example of what can be expected, Figure 3 shows the spectrum of natural radioactivity which was recorded at the CHOOZ detector site using an NaI crystal[6]. The highest energy peak, due to Th, is located at 2.6 MeV. Thus a 3 MeV minimum visible energy cut will eliminate these events.

The U and Th from the detector phototubes and walls is further reduced by cutting on distance from the fiducial volume. Assuming a 10 cm standoff, the PMTs are 1.3 m away from the edge of the fiducial volume. On the basis of this, we will assume there are negligible background from the tubes and walls of the detector.

The U and Th in the scintillator represents a potential background, although it should be very small after the 3 MeV cut is applied. However, it is wise to measure this rate, which can be done in three ways. First, one can extrapolate from the region below 3 MeV to estimate the tails. Second, the rate can be measured if there are reactor off periods. Lastly, ex-situ measurement can be made at an underground counting facility. If, through all of these measurements one is still not satisfied, the $E_{vis\ min}$ cut can be adjusted. For this study we will assume the U and Th backgrounds in scintillator are zero after the $E_{vis} > 3$ MeV cut.

5.2 Michel Electron Background

The ratio of stopping to through-going muons at 300 mwe has been calculated to be 7×10^{-3} [16]. The flux of cosmic rays entering a detector under 300 mwe overburden, as obtained by CHOOZ, is $0.4/\mathrm{m}^2/\mathrm{s}$. Hence the stopping rate in the detector is: $0.003/\mathrm{m}^2/\mathrm{s}$. The fiducial region of the generic detector is 1.5 m, thus the stopping rate is 0.02 Hz, or about 2×10^6 Michel decays for the run.

Background from muon decay is removed by the 22 μs look-back and by energy cuts. The look-back system alone reduces the background to 4.5×10^{-5}. We achieve more than a factor of 0.01 more by the $3 < E_{vis} < 5$ MeV cut, since the Michel electron energies peak at ~ 50 MeV. Therefore, we take the number of background events from this source to be negligible.

5.3 Neutrons

Cosmic rays can produce spallation neutrons either outside or within the tank, but these are a negligible background. This is because these neutrons, like unassociated neutrons described above, will fail the energy window. H captures result in energy which is below 3 MeV and Gd captures result in energy above 5 MeV. Moreover, for neutrons which enter the tank, the n must traverse 6.7 interaction lengths (40 cm) of Gd doped scintillator in order to reach the fiducial volume. The resulting rejection is about 0.001. Therefore, we take this background to be negligible in this study.

5.4 Stopping-muon-induced 12B

Cosmic ray muons entering the detector may capture and produce ^{12}B which β decays. Capture occurs 8% of the time in oil [13]. Because only the μ^- captures, we gain a factor of two. Thus the rate of stopping muons which capture is $0.02\mathrm{Hz}\times0.04 = 0.0008$ Hz. However, less than 20% of these events appear in the $3 < E_{vis} < 5$ window. Thus, the rate is less than 0.00016 Hz.

This background can be further reduced by a factor of two by introducing a look-back system of one lifetime, or 40 ms, for the parent cosmic ray. 14% of the ^{12}B events would survive such a look-back system. The cosmic ray flux through the 1.5 m radius fiducial volume (7 m^2 area) is $0.4/\mathrm{m}^2/\mathrm{s}$ or 2.8 Hz. Thus a 40 ms look-back introduces a 11% dead-time, which is acceptable.

Isotope	1/2 life (s)	Endpoint	Rate (1/d)	with Cut (1/d)
^{11}Be	13.80	11.5	< 2	< 0.4
^{9}Li+^{8}He	0.18 & 0.12	13.6 & 10.6	2	< 0.4
^{8}Li	0.84	16.0	4	< 0.5
^{6}He	0.81	3.5	14	< 2.0
^{9}C	0.13	16.0	4	< 0.5
^{8}B	0.77	13.7	4	< 0.6

Table 3: Isotopes with energy endpoint > 3 MeV. Rates are for the CHOOZ II 10 ton PXE detector[17]: 10 tons fiducial volume with 300 mwe overburden. Approx. rate with cut refers to the expectation when the $3 < E_{vis} < 5$ MeV window is applied. Top table: β^- production; bottom table: β^+ production

Implementing this result in a rate of 2×10^{-5} Hz or 1555 events per detector. Thus the total background from this source is 3110 events.

5.5 High-energy-muon-induced Isotopes

High energy cosmic rays may also produce isotopes through spallation. The rates for a 10 ton detector located under a 300 mwe overburden have been calculated by the CHOOZ II collaboration[17]. These rates were based on results from the NA54 experiment at CERN which studied isotope production from ^{12}C using 100 and 190 GeV muon beams[18]. The rates for isotopes which produce energy above 3 MeV are listed in Table 3, column 3. For those isotopes listed, the systematic error on the measurement is small [17] and will not be considered.

By taking the fraction of events in a 2 MeV window, assuming a flat distribution, we obtain the approximate rate with energy cut. This may an overestimate since the β spectrum rises rapidly near the peak; hence the less-than symbol. In principle the events producing a β^+ can be removed via an event topology analysis, but this is a small improvement and so it is not applied here. Our two detectors each have fiducial volume approximately equal to the CHOOZ II 10 ton detector. Therefore, we double the estimate in the table to obtain a background rate of less than 9 events/day. This gives an upper limit of 8100 events in the full run. This background is roughly equal in size to the signal and is a major concern for the experiment.

We note that these rates may be overestimates. Reference [19] indicates that a lower rate of ^{9}Li has been observed at KamLAND than was expected. This bears further investigation.

It is important to investigate methods for reducing this background. These isotopes are long-lived and the cosmic ray rate is 2.8 Hz/detector, rendering a look-back veto system unfeasible due to the deadtime. Instead, it is necessary to find a method for identifying only those cosmics which caused spallation. This will represent a much lower event rate and hence introduce only a small loss of live-time. The spallation event might be tagged by the combination of a muon followed by capture of the spallated neutron(s). Using methods such as this, the rate of isotope production may be reduced by more than an order of magnitude [19].

5.6 Comment on the Need for 300 mwe Overburden

With 300 mwe overburden, we have estimated the total background rate during the run to be $N_{env} = 11,200$ events. This enters into the calculation of the error on the background as $\sqrt{N_{env}}/N_e$, where N_e is the number of elastic scatters, and is about 0.2%. This represents the limit of what is acceptable for a measurement comparable to NuTeV.

The backgrounds from muon-induced events are intolerable for shallower depths. For example, for 37.5 mwe, which is among the lowest of the proposed depths for the CHOOZ II near detector, the β-decays from isotopes produced by high energy muons rises by an order of magnitude [17]. The ^{12}B rate increases by more than an order of magnitude because the muon stopping-to-through going rate is significantly higher at shallower depths[16]. Hence the fractional error at shallow depths is over a factor of three higher than at 300 m. In section 7, we address the capability of this experiment at a depth of 37.5 mwe.

6 The $\bar{\nu}p$ Normalization Sample

The $\sin^2\theta_W$ measurement requires that the absolute $\overline{\nu}_e$ flux be known with good accuracy. The flux can be measured in a straightforward manner using the high statistics sample of $\overline{\nu}p$ inverse beta-decay events. These events have a very well known cross section versus energy, and can be isolated using the coincidence signal of an outgoing positron plus an outgoing neutron. For the $\overline{\nu}p$ events, the incident neutrino energy is directly related to the visible

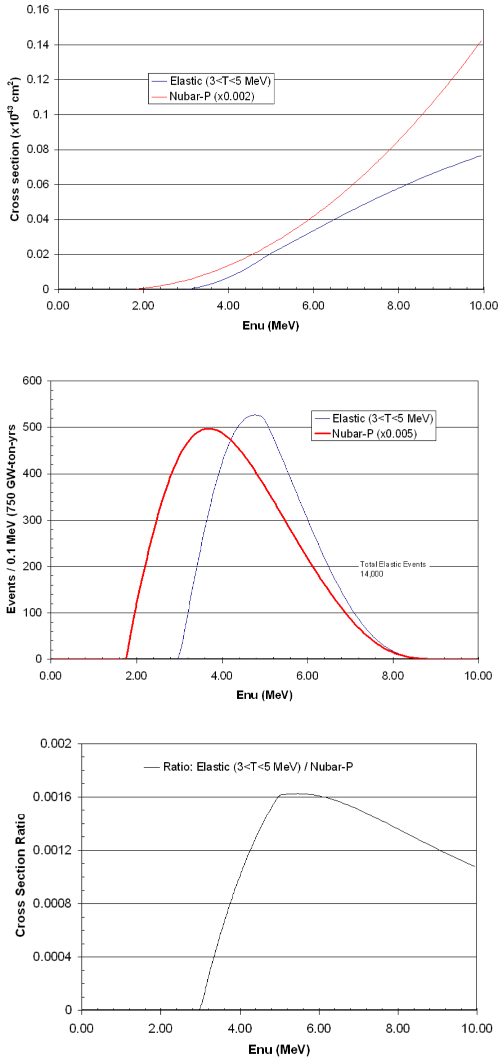

Figure 7: Top: Comparison of the $\bar{\nu}e$ cross section with $3 < E_{vis} < 5$ MeV to the scaled $\bar{\nu}p$ cross section with no visible energy cut; Center: Event rates for $\bar{\nu}e$ and $\bar{\nu}p$, scaled; Bottom: Ratio of cross sections, which is the correction function (see text)

energy through the relation

$$E_\nu = E_{vis} + 1.8 - 2m_e$$

The $\overline{\nu}p$ inverse beta-decay cross section is also very well known from measurements of the neutron lifetime which has an uncertainty of 0.2%. Thus, a measurement of the number of the $\overline{\nu}p$ events gives a direct determination of the $\overline{\nu}_e$ flux in a fiducial volume similar to the $\overline{\nu}_e e$ events.

The $\overline{\nu}p$ inverse beta-decay events can also be used to predict the number of $\overline{\nu}_e e$ events by weighting by the relative cross section as a function of energy. As described previously, the $\overline{\nu}_e e$ events will be accepted in a visible energy window between $3 < E_\nu < 5$ MeV; the relative cross section, therefore, needs to include this requirement. Figure 7 (top) shows the cross sections for elastic scattering with the $3 < E_\nu < 5$ MeV requirement and inverse beta decay as a function of incident neutrino energy. Note a scaling factor of 0.002 is applied to conveniently show both cross sections on the same plot. The middle plot, which is also scaled for convenience, compares the number of events for the two processes. Figure 7 (bottom) shows the ratio of the cross sections, which is the correction function.

The error in the $\overline{\nu}_e e$ event prediction as a function of $\sin^2\theta_W$ has contributions from statistical and systematic uncertainties. The statistical uncertainty is related to the $\overline{\nu}p$ inverse beta-decay event sample used to determine the flux. For the assumed "generic experiment" described here, there will be more than 1×10^6 inverse beta-decay events which when weighted by the cross section ratio of $\overline{\nu}_e e$ to $\overline{\nu}p$ interactions is reduced by about 0.7%. Thus, the statistical error associated with the flux normalization and energy dependence will be small.

An important systematic error associated with the normalization is the number of free protons in the oil, which is correlated to the number of electrons available as targets for elastic scattering. In fact, the fractional error on the number of electrons is 75% of the error on the number of free protons. CHOOZ determined the number of free protons by burning the oil [6], yielding a measurement accurate to 0.8%. Assuming we can do no better, the fractional error on the number of electrons is, therefore, 0.6%.

Another important systematic is the error on the fraction of neutrons which will be tagged by a Gd capture. As discussed in section 1, we use this sample because it selects events with negligible background. We assume that $84 \pm 0.7\%$ events will capture on Gd. This is a significant error in the analysis and must be reduced if possible.

Background	Rate	Comment
$\bar{\nu}p$ events,	0.05%	Event Topology Analysis applied
$\bar{\nu}p$ events	0.26%	No Event Topology Analysis
^{12}B	3110	900 live-days
Spallation-induced isotopes	11,200	900 live-days
U, Th, cosmic rays, Michel electrons	0	

Table 4: Summary of the rates assumed for backgrounds in calculation of the error on $\sin^2\theta_W$.

The event topology analysis can also be used to reduce the error on the fraction of Gd captures by more than a factor of 2, by providing an alternative method for measuring this fraction. As can be seen from Figure 6, one can isolate a pure sample of well-identified $\bar{\nu}p$ interactions without recourse to neutron identification. With a very hard cut of $\chi^2 > 0.065$, one obtains a very pure sample of events containing positrons, and retains more than 10^5 events. Thus the statistical error associated with this measurement is small. A 3.1% correction must be applied for contamination of the sample by events outside of the neutron delay time window. The systematic error associated with this correction is negligible since the neutron capture lifetime is straightforward to measure with high precision in the detector. Once the sample is corrected, the fraction which capture on Gd can be extracted by the associated γ's. Thus this method will yield a measurement which is better than 0.5%. We note that the small inefficiency on H capture can also be measured with this technique.

In calculating the error on $\sin^2\theta_W$, we will consider two cases. The first assumes the error on the Gd capture fraction is 0.7%. The second assumes the event topology analysis is proven successful and this error is reduced to 0.35%.

7 Calculating the error on $\sin^2\theta_W$

We first obtain the error on the number of signal events and then extract the error on $\sin^2\theta_W$. The terms which contribute to the error on the number of signal events are: 1) the statistical error on the signal; 2) the statistical and systematic errors associated with the $\bar{\nu}p$ background; 3) the statistical

Statistical error on the signal	0.9%
Statistical error $\bar{\nu}p$ background subtraction	0.2%
Systematic error $\bar{\nu}p$ background subtraction	0%
Statistical error on environmental background subtraction	0.9%
Systematic error on environmental background subtraction	0%
Statistical error on the normalization	0.1%
Systematic error on electron-to-free-proton ration	0.6%
Systematic error on the Gd capture fraction	0.35%

Table 5: Fractional errors contributing to the error on the number of $\bar{\nu}e$ scattering events based on assumptions presented in this paper. This table assumes the Event Topology Analysis was applied, as discussed in section 7.1.

and systematic errors associated with the environmental backgrounds; and 4) the statistical and systematic errors associated with the normalization. The total rates for the various potential backgrounds is summarized in Table 4.

For the first calculation, we assume that an event shape analysis is successful at the level discussed in section 4.5. For the second calculation, we find the error if no event topology analysis is applied. Next, we consider what is required to reach the NuTeV level of error. Lastly, we examine the effect on the error of having a 37.5 mwe overburden.

7.1 Using an Event Topology Analysis

In this section, we consider the contribution of each error source, assuming an event topology analysis has been applied. A summary of each of the sources, along with the fractional error on the number of $\bar{\nu}e$ events, is shown in Table 5.

The statistical error on the signal is calculated using the number of elastic scattering events within the $3 < E_{vis} < 5$ MeV window, $N_{e\ tot}$. The efficiency for reconstructing $\bar{\nu}e$ events, ϵ_e is 85% as discussed in section 4.5. Therefore the livetime is increased from 900 to 1035 days. The number of events for this analysis is $N_e = N_{e\ tot}\epsilon_e$ and the statistical error term is $\sqrt{N_e}/(N_e)$. We find that for 1035 days live-time, $N_e = 13,155$ events and the fractional error is 0.9%.

The statistical error from the $\bar{\nu}p$ background subtraction is $\sqrt{N_{p\ bkgd}}/N_e$. $N_{p\ bkgd}$ is given by the number of $\bar{\nu}p$ events passing the signal cuts, N_p, multiplied by the inefficiency for identifying these events correctly, ϵ_p. For 1035 days live-time, $N_p = 1,408,049$. In this analysis, the inefficiency is 0.05%, as discussed in section 4.5. Thus $N_{p\ bkgd} = 70,402$ events and $\sqrt{N_{p\ bkgd}} = 265$ events. Therefore, $\sqrt{N_{p\ bkgd}}/N_e$, the fractional error from the statistical error on the background subtraction is 0.2%. We assume that the systematic error on the $\bar{\nu}p$ background measurement is negligible (see section 4 for justification).

Only statistical errors from subtraction of the environmental backgrounds are considered here. The total environmental background is estimated $N_{env} = 11,200*1.15 = 10,000$ events, where the we have accounted for the 15% extra run time for an event topology analysis. This enters as $\sqrt{N_{env}}/N_e = 0.9\%$.

The statistical error on the normalization sample is extracted using $N_{n\ eq}$, the number of equivalent $\bar{\nu}p$ events weighted by the cross section ratio (see section 6). We find that $N_{n\ eq} = 1,334,930$. For the setup we describe, this must be adjusted by 84%, since the normalization sample uses only events which capture on Gd. The fractional error coming from the statistics of $\bar{\nu}p$ events used in the normalization is 0.1%.

The first systematic error on the normalization sample comes from knowledge of the number of electrons in the sample, As discussed in section 6, this is tied to the knowledge of the number of free protons and is $dN_{free\ p}/N = 0.6\%$.

The second significant systematic error on the normalization sample comes from the error on the knowledge of the Gd capture fraction. Assuming that an event topology analysis improves this knowledge over what was attained at CHOOZ, this is $dN_{Gd\ ratio}/N = 0.35\%$.

Adding the systematic errors in quadrature, we find $(dN/N)_{sys} = 1.0\%$. Adding this in quadrature with the statistical error on the signal yields $(dN/N)_{tot} = 1.4\%$. This is close to the goal of 1.2% which we set at the start of this paper. Extracting the error on $\sin^2\theta_W$, we obtain: $\delta(\sin^2\theta_W) = 0.0020$.

7.2 Using No Event Topology Analysis

If an event topology analysis is not used, then there is higher $\bar{\nu}p$ background contamination. Also, the Gd capture ratio is less well determined, adding a significant error to the normalization. The following assumptions change:

- 900 days livetime
- $\epsilon_e = 100\%$

- $\epsilon_p = 0.3\%$
- $dN_{Gd\ ratio}/N = 0.7\%$

The result is that the error on $\sin^2\theta_W$ rises to $\delta(\sin^2\theta_W)$=0.0022. This is a small change because the inverse beta decay backgrounds do not dominate the errors.

7.3 Scenario Which Achieves the NuTeV Error

The scenario which matches the NuTeV absolute error employs both an event topology analysis and a spallation neutron veto. The latter addressed the error from isotopes produced by spallation, which are significant in this analysis. As discussed in section 5.5, it may be possible to reduce this through a look-back for cosmics followed by spallation neutron capture. If this veto were to reject 90% of the spallation-related isotope decays without introducing an intolerable deadtime then the error, in the case where a shape analysis is applied, is $\delta(sin^2\theta_W) = 0.0017$.

7.4 A 37.5 mwe Overburden

If the overburden is 37.5 mwe, then, as addressed in section 5.6, the event rate from muon production of β-decaying isotopes rises by more than an order of magnitude. If we assume only a factor of 10 increase, then during the run there would be more than 1×10^{-6} background events from this source. Using this rate and not applying an event topology analysis yields $\delta(sin^2\theta_W) = 0.0038$. This is not competitive with other measurements in this Q^2 range. Hence, a larger overburden is required.

8 Conclusions

This paper discusses a technique for measuring $\sin^2\theta_W$ at a reactor-based experiment using $\bar{\nu}e$ elastic scatters. We have used an experimental design which is consistent with many proposals for near detectors at reactor-based oscillation experiments. We have also assumed realistic reactor power and a human-scale run time of about 900 days.

The analysis has statistical and systematic errors which are roughly equal. Therefore increased statistics can yield further improvement. At least $\sim$25 tons of fiducial volume are required and the detector should be located as close as possible to the reactor (~ 250 m or less).

We have also considered backgrounds from misidentified inverse beta decay events. Using n-identification and a visible energy window, this background can be reduced to an acceptable level. However, an event topology analysis to differentiate $\bar{\nu}p$ events from $\bar{\nu}e$ events looks promising for providing further reduction.

Environmental background is dominated by the contribution from spallation by cosmic ray muons which produce isotopes which β-decay. To attain acceptable rates, 300 mwe overburden is required. At 37.5 mwe, the backgrounds rise by over an order of magnitude. Future studies on reducing this background by identifying muons which spallate are important. A combined event topology analysis and a look-back to veto on cosmics with spallation neutrons yields an error equivalent to NuTeV.

We have also introduced the idea of normalizing to the $\bar{\nu}p$ events. This substantially reduces the error from the flux. The error which dominates the analysis presented here is due to the Gd capture ratio. This will not enter if captures on both H and Gd events are accepted. However, the backgrounds which enter the normalization sample due to including H captures will need to be addressed.

The total error which can be obtained on $\sin^2\theta_W$ using the event topology analysis method is: $\delta(\sin^2\theta_W)$=0.0020. This is comparable to the NuTeV error of 0.0017. If an event topology analysis is not used, then the error rises to $\delta(\sin^2\theta_W)$=0.0022. In both cases, the error is lower than the published SLAC E158 and APV errors.

This exercise was meant to serve as a proof-of-principle that a reasonable error on $\sin^2\theta_W$ can be attained at a reactor-based experiment. Certain aspects of the analysis have been simplified. For example, the systematic errors on the backgrounds have not been evaluated. Also, energy resolution was not considered. These will add to the error in the experiment when they are evaluated, but they are expected to be small.

On the other hand, several improvements can further reduce the error presented here. First, the analysis has roughly equal contributions from statistical and systematic sources. Increased rate can be obtained in a number of ways, including longer run time, larger or more detectors, closer position to the reactor, higher reactor power, etc. Second, the level of muon-induced background was overestimated in this study. A careful analysis using the proper energy distribution for each decay could reduce this background by as much as a factor of two. Third, the event topology analysis, which looks promising in its toy form, must be developed into a more accurate model. Lastly, the error from selecting only Gd events for the normalization can be eliminated by using all n-identified events. This comes at the cost of some background in the normalization sample, which must be estimated. However, it is possible that this introduces a smaller error than the Gd capture ratio.

In conclusion, a measurement of $\sin^2\theta_W$ at a reactor-based experiment may well be able to attain comparable errors to the NuTeV experiment. This measurement is important for testing the NuTeV anomaly using a method with substantially different systematics. Therefore, we conclude that more detailed studies are warranted.

Acknowledgments

We thank G. P. Zeller, J. Link, and the Columbia Neutrino Group for useful discussions. We thank B. Roe for the code on which the toy Monte Carlo for the event topology analysis is based.

References

[1] G. P. Zeller *et al.*, Phys. Rev. Lett., 88 (2002) 091802.

[2] S. C. Bennett and C. E. Wieman, Phys. Rev. Lett, 82 (1999) 2482.

[3] K. Bega *et al.*, hep-ex/0209017.

[4] http://www.slac.stanford.edu/exp/e158/

[5] F. Reines, H.S. Gurr, and H. W. Sobel, Physical Review Letters, 37:6 (1976) 315.

[6] M. Appollonio *et al.*, hep-ex/0301017.

[7] K. Anderson *et al.*, available at http://www.hep.anl.gov/minos/reactor13/white.html

[8] Z. Daraktchieva *et al.*,Phys. Lett. B564 (2003) 190.

[9] A. Baldini *et al.*, Nuc. Inst. Meth., A389 (1997) 141.

[10] C. Bemporad, G. Gratta, and P. Vogel, Rev. Mod. Phys. 74 (2002) 297.

[11] O.J. Smirnov, IFN/TC-00/17.

[12] K. Eguchi *et al.*, hep-ex/0212021.

[13] A.A. Aguilar-Arevalo *et al.*, available at http://www-boone.fnal.gov/publicpages/news.html

[14] D.H. Wilkenson, Nucl. Phys., A377 (1982) 474.

[15] Y. Kino *et al.*, J. Nuc. Rad. Sciences, 1:2 (2000) 63.

[16] G.L. Cassiday, J.W. Keuffel, and J.A. Thompson, Phys. Rev. D, 7:7 (1973) 2022.

[17] T. Lasserre, Talk Presented at the 2nd International Workshop on Future Reactor Neutrino Experiments, Munich, Oct. 9, 2003.

[18] T. Hagner, *et al.*, Astropart. Phys. 14 (2000) 33.

[19] G. Horton-Smith, J. Atwell, and R.D. McKeown, P. Vogel, Talk Presented at 2nd International Workshop on Future Reactor Neutrino Experiments, Munich, Oct. 9, 2003.